Monte Carlo-Based Analytical Models for Electron and Hole Electrical Parameters in Strained SiGeC Alloys

Marc Michaillat*†, Denis Rideau*, Frédéric Aniel†, Clément Tavernier*, Hervé Jaouen*

*STMicroelectronics, 850, rue Jean Monnet, 38926 Crolles FRANCE
†IEF - CNRS UMR 8622, Bât. 220, Université Paris-Sud, 91405 Orsay FRANCE

***Abstract*—Bipolar transistors in advanced BiCMOS technology rely on highly-doped SiGeC bases strained on Si. Modeling the electrical properties of such devices by TCAD means requires an accurate description of SiGeC transport parameters, including low-field mobility, saturation velocity and energy relaxation time. Since bipolar transistor operation involves electron and hole transport, both types of carriers must be adressed. A distinction between majority and minority carriers must also be physically accounted for. In this paper, transport properties of doped and strained $Si_{1-x-y}Ge_xC_y$ alloys are investigated by Full-Band Monte Carlo (MC) method with a view of deriving analytical models suitable for implementation in hydrodynamic-based TCAD simulators.**

I. Introduction

Performance optimization of advanced heterojunction bipolar transistors (HBTs) has lead to the introduction of germanium and carbon in the device base, yielding $Si_{1-x-y}Ge_xC_y$ base layers biaxially strained on Si [1]. TCAD simulation of charge carrier transport in such SiGeC/Si HBTs should include models for transport parameters relevant to strained ternary $Si_{1-x-y}Ge_xC_y$ alloys. The aim of this work is to develop analytical models for carrier transport parameters, namely low-field mobility and energy relaxation time, based on Monte Carlo simulations of homogeneous transport in SiGeC alloys.

II. Monte Carlo Method

Our Full-Band Monte Carlo simulations rely on strain-dependent SiGe Tight-Binding band structures. Phonon scattering rates are wave-vector dependent [2] and include 4 Si-Si modes and 4 Ge-Ge modes (i.e. 8 phonon modes in SiGeC alloys) [3]. Phonon rates are calibrated to reproduce a large number of experimental data in bulk Si and Ge, namely low-field mobility, drift velocity and impact ionization coefficient measurements [4], [5]. Doping effets are accounted for using doping-dependent scattering mechanisms, including ionized impurity scattering, electron-electron scattering and electron-hole scattering. Coulombian scattering rates are derived from partial-wave theory [6], [7] and can thereby establish a physical distinction between attractive and repulsive potentials, i.e. between majority and minority carriers (Fig.1). The Pauli Exclusion Principle (PEP) has to be accounted for

TABLE I
Effective alloy potentials expressed in eV
[a] from [9], [b] from [10], [c] from [3], [d] from [11], [e] from [12]

REF	U_{Si-Ge}		U_{Si-C}	
	e	h	e	h
Present work	0.4	0.5	2.8	2.2
Litterature	0.7[a], 0.54[b]	0.9[a], 0.7[c], 0.55[d]	1.75[e]	–

in simulating highly doped materials. Here PEP is included using the actual distribution function discretized with a cubic mesh of the reciprocal space [8]. Eventually our model for alloy scattering extends the commonly used alloy scattering rate model specific to binary random alloys (see e.g. [3], [9]) to the more general case of ternary random alloys:

$$P_{alloy}(x,y,E) = \frac{2\pi}{\hbar}\Omega_c \cdot \mathcal{D}(E) \cdot \Big[x(1-x) \cdot U^2_{Si-Ge} + y(1-y) \cdot U^2_{Si-C} - 2xy \cdot U_{Si-Ge} \cdot U_{Si-C}\Big] \tag{1}$$

In (1), U_{Si-Ge} and U_{Si-C} are effective alloy potentials. As such they are independently calibrated on several experimental mobility measurements:

- U_{Si-Ge} is adjusted to reproduce the x dependence of mobility in relaxed $Si_{1-x}Ge_x$ alloys, as depicted in Fig.2;
- U_{Si-C} is tuned to reproduce the y dependence of in-plane mobility in $Si_{1-y}C_y$strained on Si, as shown in Fig.3.

Table I compares the calibrated values of our SiGeC model with equivalent effective alloy potentials avaible in the litterature, relevant to binary SiGe and SiC alloys. It ought to be noted that using (1), our model provides a unified formalism for electrons and holes in strained and relaxed ternary SiGeC.

III. Mobility Model

A large set of MC simulations have been performed in highly-doped $Si_{1-x-y}Ge_xC_y$ alloys strained on Si. First, we have derived a new anisotropic analytical mobility model based on low-field MC simulations. The model should be valid for materials with up to 2% carbon content and 50% germanium content. It should also be able to distinguish between the isotropic relaxed mobility, and the in-plane and

978-1-4244-3947-8/09/$25.00 ©2009 IEEE

out-of-plane components of the anisotropic mobility tensor relevant to SiGeC alloys strained on bulk Si.

In order to account for strain-related effects, we introduce a strain-compensation parameter z, defined as:

$$z = y - 0.1071x - 0.0163x^2 \tag{2}$$

z is positive (negative) when the SiGeC alloy is tensily (compressively) strained on Si and $z = 0$ when the alloy is exactly strain-compensated. The alloy composite mobility is modeled through the introduction of bowing parameters, as described in Ref.[13]:

$$\frac{1}{\mu} = \frac{1-x}{\mu^{Si}} + \frac{x}{\mu^{Ge}} + \left[\frac{x(1-x)}{C_x^0 + xC_x^1 + x^2C_x^2} + \frac{y(1-y)}{C_y} - \frac{xy}{C_{xy}}\right]\frac{1}{C_\beta(z)} \tag{3}$$

where the bowing terms C_x^i, C_y and C_{xy} quantify the degradation of mobility due to alloy scattering. In (3), both μ^{Si} and μ^{Ge} mobility terms are described using doping-dependent Caughey-Thomas expressions [14]. All model parameters are adjusted to obtain an optimal agreement between formula (3) and MC simulations results.

Figure 4a (4b) shows the behavior of the resulting majority (minority) electron mobility in SiGe alloys as the doping concentration is increased. Figures 5a to 5d show the dependence of electron mobility upon C content in intrinsic biaxially strained SiGeC alloys. This mobility model is seen to satisfactorily reproduce all effects due to substitutional C, namely alloy scattering, anisotropy due to biaxial strain, and strain compensation when Ge is also introduced (arrow in Fig.5c).

In order to underline the effects of Ge and C contents on the alloy mobility, it is useful to plot the ratio between SiGeC mobility and Si mobility:

$$R_\mu = \frac{\mu(x,y)}{\mu^{Si}} \tag{4}$$

The mobility ratio R_μ can be conveniently used to identify domains of the (x, y) composition spectrum where mobility enhancements could be expected as compared to Si. In figures 6 and 7, we plot the ratio R_μ for several doping concentrations, as given by the analytical law (3). The figures show the isolines of the ratio in the $x - y$ alloy composition space. Fig.6 relates to electron in-plane mobility, while Fig.7 depicts hole in-plane mobility. As it can be seen, electron mobility in strained $Si_{1-x-y}Ge_xC_y$ alloys is always lower than mobility in Si ($R_\mu < 1$), since the beneficial strain effects induced by lattice mismatch cannot overcome the strong alloy scattering. However in the case of hole mobility, both those competing trends, namely alloying and strain, can result in a very significant mobility enhancement ($R_\mu > 1$), especially when the SiGeC layer is submitted to a highly compressive biaxial stress.

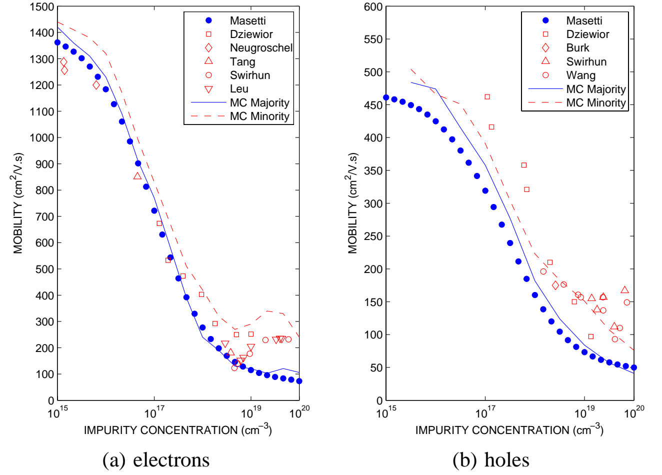

(a) electrons (b) holes

Fig. 1. Mobility as a function of impurity concentration in silicon. MC simulation results are compared to measurements. Full (open) symbols and solid (dashed) lines refer to majority (minority) carrier mobility. Experimental data are taken from Ref.[15], [16], [17], [18], [19], [20], [21], [22], [23], [24], [25].

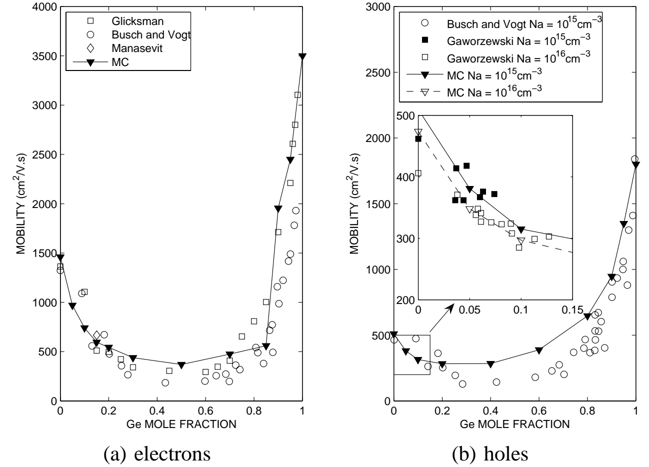

(a) electrons (b) holes

Fig. 2. Mobility as a function of Ge content in relaxed SiGe alloys. MC simulation results are compared to measurements. Experimental data are taken from Ref.[26], [27], [28], [11].

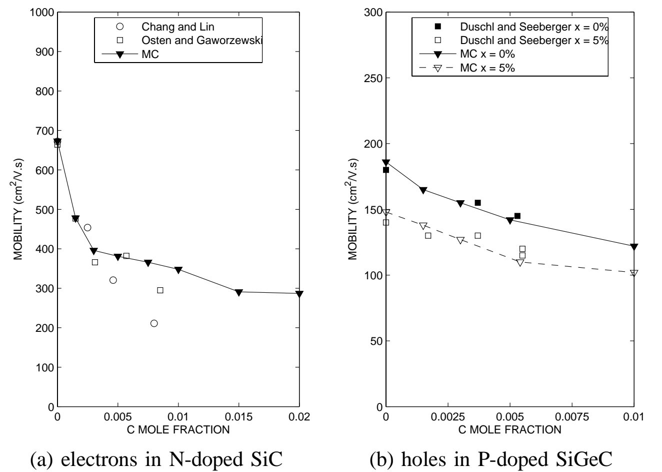

(a) electrons in N-doped SiC (b) holes in P-doped SiGeC

Fig. 3. In-plane mobility as a function of C content in SiGeC alloys strained on Si. MC simulation results are compared to measurements. Experimental data are taken from Ref.[12], [29], [30].

TABLE II
PARAMETER VALUES FOR THE ENERGY RELAXATION TIME MODEL

CARRIER	τ_0 ps	τ_1 ps	C_0
e	0.38	0.04	0.18
h	0.36	0.13	0.10

IV. ENERGY RELAXATION TIME MODEL

In a second set of Full-Band MC simulations, high-field transport properties such as saturation velocities and energy relaxation times are investigated. The energy relaxation time is extracted using the indirect method reported in Ref.[31]. During constant-field MC simulations, charge carrier drift velocity v_c and average energy E_c are calculated. The carrier energy relaxation time is deduced from the 2 aforementioned pieces of data, according to:

$$\tau = \frac{3k_B}{2e} \times \frac{T_C - T_L}{v_c F} \tag{5}$$

where F is the electric field, T_L is the lattice temperature, and the carrier temperature T_C is related to the carrier energy E_c through $E_c = 3/2k_B T_C$.

Starting from the MC results, we develop and calibrate an analytical formula for the carrier energy relaxation time in $Si_{1-x-y}Ge_xC_y$ alloys. It is found that the relaxation time τ can be efficiently modeled as a function of the ratio between carrier temperature T_C and lattice temperature T_L [31]:

$$\tau = (\tau_0 + \tau_1 x) \times \left[1 - \exp\left(-C_0 \frac{T_C}{T_L}\right) + \left(\frac{T_C}{T_L}\right)^{-1}\right] \tag{6}$$

In (6), the τ_1 parameter controls the alloying effect due to Ge mole fraction x. The dependencies of τ upon C mole fraction and doping concentration were found to be negligible. Model parameter values specific to electron and hole transport are reported in table II.

Figures 8a and 8b show MC results for the electron and hole energy relaxation time in SiGe alloys, respectively. Also shown is the analytical model behavior, as expressed in (6). As it can be seen, the MC-based model significantly improves the default constant model commonly used in device simulations.

V. CONCLUSION

We have employed a homogeneous Monte Carlo simulation technique to calculate charge carrier transport properties in ternary $Si_{1-x-y}Ge_xC_y$ alloys. All the relevant scattering mechanisms have been included, and their respective scattering rates have been modeled consistently with a large number of experimental measurements. Analytical models for electron anf hole low-field mobility and energy relaxation time have been derived from a systematic fitting procedure applied to Monte Carlo results. Based on the presented analytical TCAD models, strategy for performance optimization in advanced bipolar devices with respect to strain and alloying effects in SiGeC, can be adequately adressed in the early phase of technology developpement.

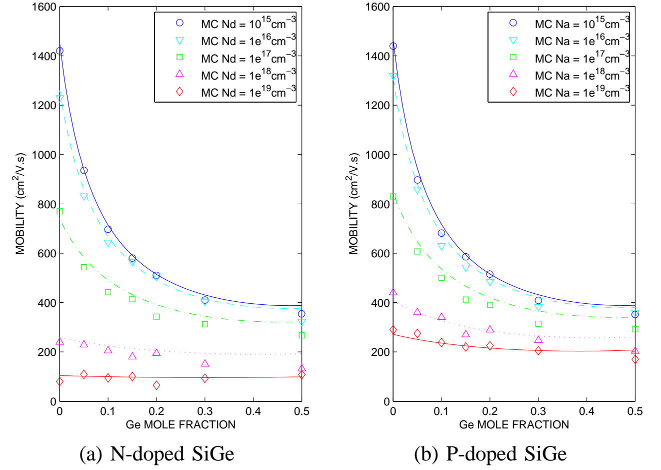

(a) N-doped SiGe (b) P-doped SiGe

Fig. 4. Combined effects of alloying and doping on electron mobility in relaxed SiGe alloys. Minority electron mobilities are consistently higher than majority electron mobilities. Symbols refer to MC simulations, lines represent our analytical mobility model.

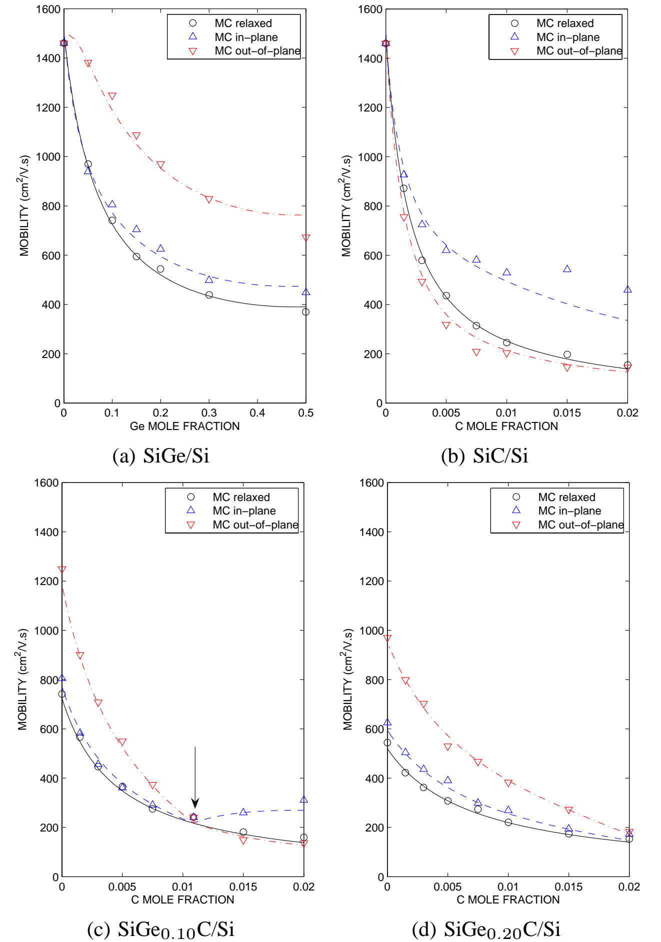

(a) SiGe/Si (b) SiC/Si

(c) $SiGe_{0.10}C/Si$ (d) $SiGe_{0.20}C/Si$

Fig. 5. Combined effects of alloying and strain on electron mobility in undoped SiGeC alloys. Biaxial strain due to lattice mismatch induces the mobility anisotropy. When strain compensation occurs, the anisotropy vanishes (arrow). Symbols refer to MC simulations, lines represent our analytical mobility model.

REFERENCES

[1] S. Decoutere and A. Sibaja-Hernandez *Mat. Sci. Semicon. Proc.*, vol. 8, p. 283, 2005.
[2] M. V. Fischetti and S. E. Laux *Phys. Rev. B*, vol. 38, p. 9721, 1988.
[3] F. M. Bufler and B. Meinerzhagen *J. Appl. Phys.*, vol. 84, p. 5597, 1998.
[4] C. Canali, C. Jacoboni, and F. Nava *Phys. Rev. B*, vol. 12, p. 2265, 1975.
[5] M. V. Fischetti, N. Sano, and S. E. Laux in *Simulation of Semiconductor Processes and Devices 1996*, p. 43, 1996.
[6] J. R. Meyer and F. J. Bartoli *Phys. Rev. B*, vol. 23, p. 5413, 1981.
[7] L. E. Kay and T.-W. Tang *J. Appl. Phys.*, vol. 70, p. 1475, 1991.
[8] P. Lugli and D. K. Ferry *IEEE Trans. Electron Devices*, vol. 32, p. 2431, 1985.
[9] M. V. Fischetti and S. E. Laux *J. Appl. Phys.*, vol. 80, p. 2234, 1996.
[10] F. Murphy-Armando and S. Fahy *Phys. Rev. Lett.*, vol. 97, p. 096606, 2006.
[11] P. Gaworzewski, K. Tittelbach-Helmrich, and U. Penner *J. Appl. Phys.*, vol. 83, p. 5258, 1998.
[12] S. T. Chang, C. Y. Lin, and S.-H. Liao *Appl. Surf. Sci.*, vol. 254, p. 6203, 2008.
[13] V. Palankovski, G. Röhrer, and T. Grasser *Appl. Surf. Sci.*, vol. 224, p. 361, 2004.
[14] D. M. Caughey and R. E. Thomas *Proc. IEEE*, vol. 55, p. 2192, 1967.
[15] G. Masetti, M. Severi, and S. Solmi *IEEE Trans. Electron Devices*, vol. 30, p. 764, 1983.
[16] J. Dziewior and D. Silber *Appl. Phys. Lett.*, vol. 35, p. 170, 1979.
[17] A. Neugroschel *IEEE Electron Dev. Lett.*, vol. 6, p. 425, 1985.
[18] D. D. Tang, F. F. Fang, and M. Scheuermann in *International Electron Devices Meeting 1986*, p. 20, 1986.
[19] S. E. Swirhun, Y.-H. Kwark, and R. M. Swanson in *International Electron Devices Meeting 1988*, p. 298, 1988.
[20] S. E. Swirhun, D. E. Kane, and R. M. Swanson in *International Electron Devices Meeting 1986*, p. 24, 1986.
[21] I.-Y. Leu and A. Neugroschel *IEEE Trans. Electron Devices*, vol. 40, p. 1872, 1993.
[22] D. E. Burk and V. D. L. Torre *IEEE Electron Dev. Lett.*, vol. 5, p. 231, 1984.
[23] S. E. Swirhun, J. A. D. Alamo, and R. M. Swanson *IEEE Electron Dev. Lett.*, vol. 7, p. 168, 1986.
[24] C. H. Wang, K. Misiakos, and A. Neugroschel *IEEE Trans. Electron Devices*, vol. 37, p. 1314, 1990.
[25] C. H. Wang and A. Neugroschel *IEEE Electron Dev. Lett.*, vol. 11, p. 576, 1990.
[26] M. Glicksman *Phys. Rev.*, vol. 111, p. 125, 1958.
[27] G. Busch and O. Vogt *Helv. Phys. Acta*, vol. 33, p. 437, 1960.
[28] H. M. Manasevit, I. S. Gergis, and A. B. Jones *Appl. Phys. Lett.*, vol. 41, p. 464, 1982.
[29] H. J. Osten and P. Gaworzewski *J. Appl. Phys.*, vol. 82, p. 4977, 1997.
[30] R. Duschl, H. Seeberger, and K. Eberl *Thin Solid Films*, vol. 336, p. 336, 1998.
[31] V. Palankovski, B. Gonzalez, and H. Kosina in *Modeling and Simulation of Microsystems 1999*, p. 395, 1999.

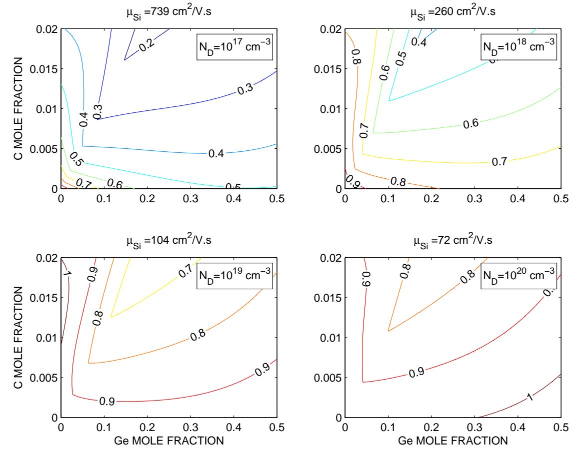

Fig. 6. Ratio between the electron in-plane mobility in strained SiGeC and the electron mobility in bulk Si, plotted as a function of Ge and C contents for 4 different donor concentrations. Isoline discontinuities are located at points of the (x, y) space where strain compensation occurs. The strain compensation points are aligned along a boundary line which separates the compressive strain domain from the tensile strain domain.

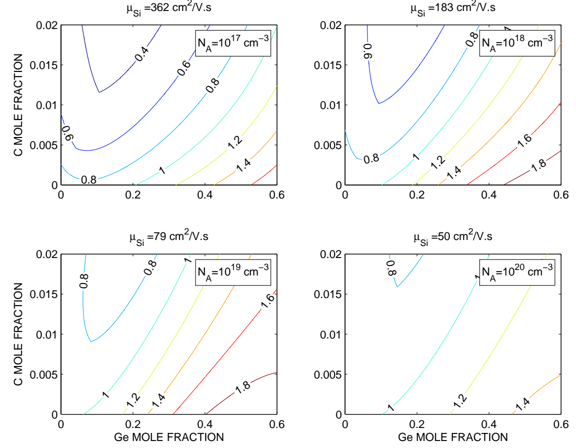

Fig. 7. Same as Fig.6 for hole mobility in acceptor-doped SiGeC and Si.

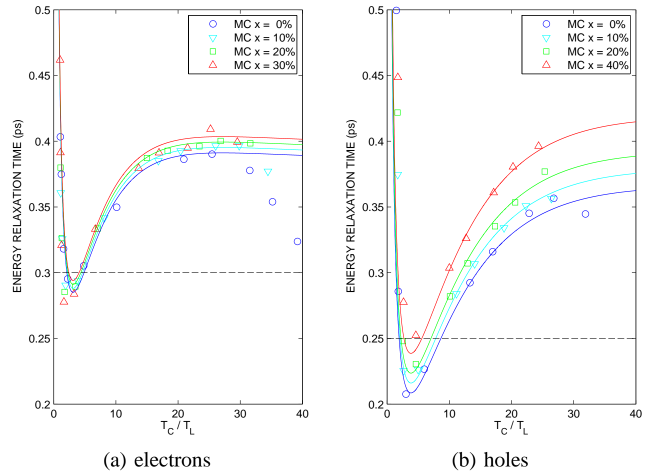

(a) electrons (b) holes

Fig. 8. Energy relaxation time as a function of carrier temperature in relaxed SiGe alloys. Symbols refer to MC simulations, solid lines represent our analytical relaxation time model. Dashed lines indicate the default relaxation time parameter values used in *Sentaurus Device* hydrodynamic model.